ELSEVIER

Applied Ocean Research 25 (2003) 243–261

Applied Ocean Research

www.elsevier.com/locate/apor

Estimating directional wave spectrum based on stationary ship motion measurements

Eduardo A. Tannuri[a,*], João V. Sparano[a], Alexandre N. Simos[a], José J. Da Cruz[b]

[a] *Department of Naval Arch. and Ocean Engineering, University of São Paulo, São Paulo, SP, Brazil*
[b] *Department of Telecommunication and Control Engineering, University of São Paulo, São Paulo, SP, Brazil*

Received 10 July 2003; revised 12 December 2003; accepted 12 January 2004

Abstract

Useful information can be derived from on-board estimation of the directional wave spectrum of the sea, especially concerning *feed forward* control of dynamically positioned systems. This work discusses the feasibility of using stationary ship motion measurements for in-site directional wave spectrum estimation, focusing on the particular problems that may arise in the application of adapted estimation methods to this kind of system. Load variations, operational trim and other disturbances frequently occur, modifying the ship response to incident waves. Since the methodology depends on previous knowledge about the amplitude response operators, these errors may cause some degradation in the estimated spectrum. Furthermore, due to the large inertia of the ship, high frequency wave components are filtered, reducing the frequency range of the spectrum that can be estimated. These drawbacks are analyzed and their influence in final estimation is quantified. Roll motion of the ship presents non-linear and resonant behavior and is extremely sensitive to load variations. For this reason, sway motion was used instead of roll one, differently from common directional buoys algorithms that take into account the three motions in the vertical plane (heave, roll and pitch). A parametric estimation method, normally used for directional buoys measurements, was adapted to the case and tested. Exhaustive numerical trials were carried out using a tanker in two loading conditions (full and ballasted) and a pipe-laying barge, under typical wave spectra of Brazil's Campos Basin, either in unimodal or bimodal cases. Small-scale towing-tank results were also used as a first experimental validation concerning unimodal unidirectional sea states. Spectral estimations based on experimental results were also compared to those obtained by means of a Bayesian estimation method presented in literature, for the sake of comparison. Parametric Method presented best accuracy in all tested cases.

Keywords: Directional wave spectrum; Estimation; FPSO

1. Introduction

As offshore oil production moves towards deeper waters, dynamic positioning (DP) systems become more and more important as an economical solution for the station-keeping of floating production units. For DP operations under extreme conditions, feed forward control may represent a significant improvement in the efficiency of the system, concerning both, station-keeping behaviour and fuel consumption. The feed forward control consists of providing information on the environmental excitation (waves, current and winds) to the system in order to predict the DP response required for counteracting the estimated environmental forces.

Wind feed forward was used since first DP systems, because the measurement of wind velocity and direction can be done by anemometers with acceptable accuracy. Wave forces feed forward control was firstly introduced by Pinkster [1], and he showed that it can lead to a significant improvement in DP performance. However, it requires the estimation of the Directional Wave Spectrum (DWS) of the sea acting on the production unit, what is the main topic of the present work.

The DWS is used to estimate the mean drift forces acting on the vessel, by means of the well-known drift

* Corresponding author current address: Escola Politécnica da USP, Departamento de Engenharia Naval e Oceânica, Av. Prof. Mello Moraes, 2231, CEP 05508-900, Cidade Universitária, São Paulo Brazil. Tel.: + 55-11-3091-5350; fax: + 55-11-3088-7989.

E-mail addresses: eduat@usp.br (E.A. Tannuri); joao.sparano@poli.usp.br (J.V. Sparano); alesimos@usp.br (A.N. Simos); jaime@lac.usp.br (J.J. Da Cruz).

0141-1187/$ - see front matter © 2004 Elsevier Ltd. All rights reserved.
doi:10.1016/j.apor.2004.01.003

coefficients of the hull. Such estimates are directly added to thrusters control forces (feed forwardloop). Of course, such estimates contain errors and also disregard the slow drift forces (zero mean low-frequency wave forces), which are compensated by the conventional control feedback loop. So, a larger part of the wave mean force is compensated by the feed forward loop, and the smaller part (which comes from estimation errors) is counteracted by a feedback loop. Since the system dynamics strongly changes for different environmental conditions, a conventional single feedback controller presents performance degradation under an environmental condition that is different from the one it was used to tune all controller parameters, which consists in a severe operational problem in commercial DPS. The association of the feedback and feed forwardloops eliminates such problem, because the feed forwardloop compensates the major part of the dynamics changes.

This paper discusses the feasibility of estimating the DWS using on on-board monitoring of the first-order motions of the unit, in particular, a FPSO (Floating Production, Storage and Offloading) system based on a moored Very Large Crude Carrier (VLCC).

In the last 30 years, sea state measurements were carried out mainly by moored directional buoys. Such devices provide good estimates of wave spectrum, since they have well known dynamics and their motions can be accurately measured by accelerometers and tilt sensors [2]. In some cases, buoys dynamics are even neglected in the numerical processing of its data, considering the measured heave, pitch and roll equal to wave height and slopes. However, buoys are easily subjected to damage and loss, and present practical and economical drawbacks related to deep water mooring system installation.

Recently, wave-monitoring radar systems have been developed based on the analysis of temporal and spatial evolution of the radar backscatter information [3,4]. These systems may be installed on board, what eliminates the problems associated to moored buoys. However, they require complex computational hardware and have a high initial cost.

The estimation of the spectrum based on ship motions measurements may overcome such problems since it requires simple instrumentation and computational hardware, and can be installed onboard. Some applications to running ships have already been described in Ref. [5–7] for example.

This paper addresses the feasibility of applying such wave monitoring system method in stationary offshore systems such as large moored tankers converted to FPSO's systems or pipe-laying barges. Of course, several problems arise in this particular case.

Concerning DP improvement by means of feed forward control, a VLCC-based FPSO certainly represents one of the most adverse applications for the methodology here proposed. In view of the ship large inertia, it does not respond to small waves. As a consequence, DWS with low peak periods cannot be estimated accurately. Nevertheless, although high frequency wave components do not excite significantly the first order motions of the ship, they may contribute significantly to the drift forces, as the ship hull reflects them.

Also, the methodology applied depends on the previous knowledge about how the ship responds to wave incidence, which is modeled by the linear Response Amplitude Operators (RAO's). However, in a FPSO several factors such as load variations, operational trim and other disturbances make the correct evaluation of the RAO's a hard task.

In such aspects, the VLCC represents a demanding test for the methodology proposed. For smaller offshore systems, such as drilling ships and barges, the drawbacks mentioned above will certainly be reduced.

Another relevant aspect to be analyzed regards the non-linear dynamic effects that also play an important role when oscillation amplitude increases. The analysis of the RAO's of a ship showed that the use of sway motion is more appropriate than roll motion, since the former does not present resonant behavior at the typical wave frequency range and is considerably less sensitive to changes in loading configurations.

A Parametric estimation method was applied to the VLCC tanker subjected to typical waves of Campos Basin, in order to test the estimation principle.

Numerical trials emulated practical problems in the estimation of RAO's, considering the full and ballasted loading condition of the FPSO. Uni and bimodal sea states were considered in the numerical analysis. Errors in the DWS and, consequently, in the wave-drift forces estimations were quantified.

A first experimental validation was obtained by estimation of the wave spectra generated at the IPT towing-tank using the motions measured on a small-scale VLCC model, subjected to such spectra. Due to tank limitations, however, only unimodal unidirectional seas could be tested.

Spectral estimations based on experimentally measured motions were also compared to those obtained by the application of a non-parametric method presented in literature, the Bayesian method. This method was chosen because it is one of the reference methods applied to directional buoys data processing [7] and has been successfully applied to running ships with no uncertainty in RAO's [8]. Furthermore, it is a non-parametric method that, in principle, is able to estimate any shape of spectrum, even bimodal cases with a swell sea associated with a random local sea. The Parametric method used considers a 8-parameter model for the spectrum as proposed in Ref. [9] and is also able to approximate bimodal spectra.

The potential of the methods is discussed and the problems that were encountered are reported.

2. Parametric estimation method

Assuming linearity between waves and ship response, the cross spectra of ship motions time series ϕ_{mn} and the DWS are related by the RAO's through the following integral:

$$\phi_{mn}(\omega) = \int_{-\pi}^{\pi} \mathrm{RAO}_m(\omega,\theta).\mathrm{RAO}_n^*(\omega,\theta).S(\omega,\theta).d\theta, \qquad (1)$$

where $\mathrm{RAO}_m(\omega,\theta)p$ denotes the Response Amplitude Operator of the motion m at frequency ω and incidence direction θ and $S(\omega,\theta)$ denotes the DWS.

The power spectrum $S(\omega)$, widely used to describe wave energy frequency distribution, may be obtained from directional spectrum by:

$$S(\omega) = \int_{-\pi}^{\pi} S(\omega,\theta)\mathrm{d}\theta$$

At this point it is worth noting that three ship motions will be considered in what follows, namely, $m = 2$ for sway, $m = 3$ for heave and $m = 5$ for pitch. Since ϕ_{mn} is real when $m =$ n and complex otherwise, Eq. (1) will give rise to 9 equalities.

By dividing the frequency range of interest $\lfloor \omega_0, \omega_f \rfloor$ in J points, $\{\omega_j\}_{j=0}^{J-1}$, the discrete expression of (1) is derived assuming the integrand to be constant on each interval $\Delta\theta$:

$$\phi_{mn}(\omega_j) = \Delta\theta \sum_{k=1}^{K} \mathrm{RAO}_{mk}(\omega_j)\mathrm{RAO}_{nk}^*(\omega_j)S_k(\omega_j), \qquad (2)$$

with $\Delta\theta = 2\pi/K, S_k(\omega_j) = S(\omega_j,\theta_k)$,

$\mathrm{RAO}_{mk}(\omega_j) = \mathrm{RAO}_m(\omega_j,\theta_k)$ and $\mathrm{RAO}_{nk}^*(\omega) = \mathrm{RAO}_n^*(\omega,\theta_k)$,

The Parametric method is conceptually simple and is based on the following 10-parameter representation of the bimodal spectrum [9]:

$$S(\omega,\theta) = \frac{1}{4}\sum_{i=1}^{2} \frac{\left(\frac{4\lambda_i+1}{4}\omega_{mi}^4\right)^{\lambda_i}}{\Gamma(\lambda_i)} \frac{Hs_i^2}{\omega^{4\lambda_i+1}} A(s_i) \times \cos^{2s_i}\left(\frac{\theta-\theta_{mi}}{2}\right) \exp\left[-\frac{4\lambda_i+1}{4}\left(\frac{\omega_{mi}}{\omega}\right)^4\right] \qquad (3)$$

where

$$A(s) = \frac{2^{2s-1}\Gamma^2(s+1)}{\pi\Gamma(2s+1)}$$

is a normalization factor for the area under a $\cos^{2s}$ curve, Γ is Gamma function, s_i represents the spreading of the ith component, Hs_i is the significant wave height, λ_i is a shape parameter, θ_{mi} is the mean direction and ω_{mi} is the modal frequency.[1] This formulation was proposed by Ref. [9] and is a combination of the 6-parameter model for the power spectrum presented in Ref. [10] (that is similar to well-known JONSWAP formulation) with the $\cos^{2s}$ model proposed in Ref. [11]. Since it considers two separated wave components (i =1 and 2), it is capable of representing a variety of spectrum shapes including bimodal spectra.

Since λ_i has weak influence on wave induced loads and ship motion, its value has been fixed as $\lambda_i = 1$. The number of parameters to estimate has then been reduced. In this case, the power spectrum related to (3) is reduced to a Pierson–Moskowitz spectrum. As will be shown in this work, even in the presence of a wave pattern in which $\lambda_i \neq 1$, the relevant parameters are well estimated with this simplification. So, the final spectrum parameterization used in the method is given by:

$$S(\omega,\theta) = \frac{1}{4}\sum_{i=1}^{2} \frac{5}{4}\omega_{mi}^4 \frac{Hs_i^2}{\omega^5} A(s_i)\cos^{2s_i}\left(\frac{\theta-\theta_{mi}}{2}\right) \times \exp\left[-\frac{5}{4}\left(\frac{\omega_{mi}}{\omega}\right)^4\right] \qquad (4)$$

The Parametric method is based on the minimization of the quadratic error of the motions predicted using the estimated spectrum and the measured ones. As already explained, the calculation is done assuming linearity between waves and ship response and uses the ship RAO's.

By using Eq. (2), for a given spectrum, the values of $\phi_{mn}(\omega_j), (0 \le j \le J-1)$ can be calculated. Denoting by $\bar{\phi}_{mn}(\omega_j), (0 \le j \le J-1)$ the measured values of the ship motions spectrum and considering the wave spectrum represented by the eight parameters of the Eq. (4), namely:

$$x = [\omega_{m1}\ Hs_1\ s_1\ \theta_{m1}\ \omega_{m2}\ Hs_2\ s_2\ \theta_{m2}]^T$$

the quadratic error may be written as

$$E(x) = \left[\sum_{m,n}\sum_{j=0}^{J-1} [\phi_{mn}(\omega_j) - \bar{\phi}_{mn}(\omega_j)]^2\right]^{1/2}$$

Thus, the spectrum estimation problem is reduced to finding the minimum point of the functional $E(x)$. The form of $E(x)$ is crucial for the convergence and the outcome from the algorithm. The uniform weight over the whole ω domain was used, since one has no prior knowledge about incident wave frequency range.

The Parametric approach is able to estimate unimodal or bimodal spectra. In both cases the method finds a 8-component vector x of estimated parameters. $x = [\omega_{m1}\ Hs_1\ s_1\ \theta_{m1}\omega_{m2}\ Hs_2\ s_2\ \theta_{m2}]^T$. For unimodal seas, one of the estimated significant heights (Hs_1 or Hs_2) is expected to be negligible.

A difficulty with the Parametric Method is that it leads to a non-linear programming problem, whose numerical solution requires a high computational effort.

[1] The modal frequency is related with the peak period T_{pi} by the expression: $T_{pi} = 2\pi/\omega_{mi}$.

Table 1
VLCC characteristics

Properties	Full loaded	~90% loaded	~80% loaded	~40% loaded	~30% loaded
Mass (M)	321900 ton	271650 ton	257500 ton	126100 ton	96680 ton
Moment of inertia (I_Z)	2.06×10^9 ton m^2	1.78×10^9 ton m^2	1.65×10^9 ton m^2	0.71×10^9 ton m^2	0.62×10^9 ton m^2
Length (L)	320 m	320 m	320 m	320 m	320 m
Draft (T)	21.47 m	19.00 m	17 m	9.00 m	7 m
Breadth (B)	54.5 m	54.5 m	54.5 m	54.5 m	54.5 m
Wetted Surf.(S)	27342 m^2	25770 m^2	24198 m^2	17910 m^2	16998 m^2

3. Sensitivity analysis

The estimation methods are strongly dependent on the RAO's used, since they contain information about ship response to incident waves.

RAO's can be obtained experimentally, either in full-scale or model-scale tests, but it is usual to apply a wave-body interaction software to perform their evaluation. Such evaluation may present some inaccuracies due to the following factors:

- *Non-linearities*—the definition of the RAO's is based on the hypothesis that the relation between wave excitation and ship response is linear. Of course, this simplification is valid for small oscillations around the equilibrium position; however, in critical situations, the ship response amplitudes may reach high values, and non-linear effects become relevant. This problem is more critical for roll motion, since it is strongly dependent on viscous forces, which are non-linear in nature. Furthermore, the large number of risers and mooring lines increase the non-linear viscous damping of the system.
- *Loading conditions*—the ship response depends on its load distribution. For the case analyzed in the present work this problem is crucial, since in a FPSO oil stored in the tanks may represent 60% of the total weight of the system. Moreover, oil free surface effects may influence ship response, although this is generally not taken into account during RAO's calculation.

In the present work, RAO's inaccuracies were emulated by uncertainties in the draft value, which are related to the second factor explained above. The method was applied to the tanker Vidal de Negreiros, a VLCC with the characteristics listed in Table 1.

RAO's were evaluated for the 5 loading conditions presented in Table 1 using a wave-body interaction software (WAMIT). For example, Figs. 1–4 show the amplitude of RAO's for a 135° wave heading incidence.

When wave spectrum estimation methods are applied to directional buoys, they normally use heave, pitch and roll motions, measured by accelerometers and inclinometers [2].

Obviously, the wave response of a buoy subjected to waves can be obtained either numerically or experimentally, since it is a small body with known parameters and dynamics. So, it can be said that its RAO's are generally known with high level of accuracy.

On the other hand, the dynamical behavior of a large body such as a VLCC tanker may be extremely difficult to be predicted and it may present high sensitivity to non-modeled effects, as previously exposed.

Indeed, for the VLCC under consideration, Fig. 4(a) confirms that roll response is strongly dependent on loading conditions, mainly due to its resonant behavior. In this case, the use of roll motion in the estimation methods would lead to non-robust results. Also, non-linear effects have much more influence in roll than in any other first-order ship motion. On the other hand sway motion presents a low

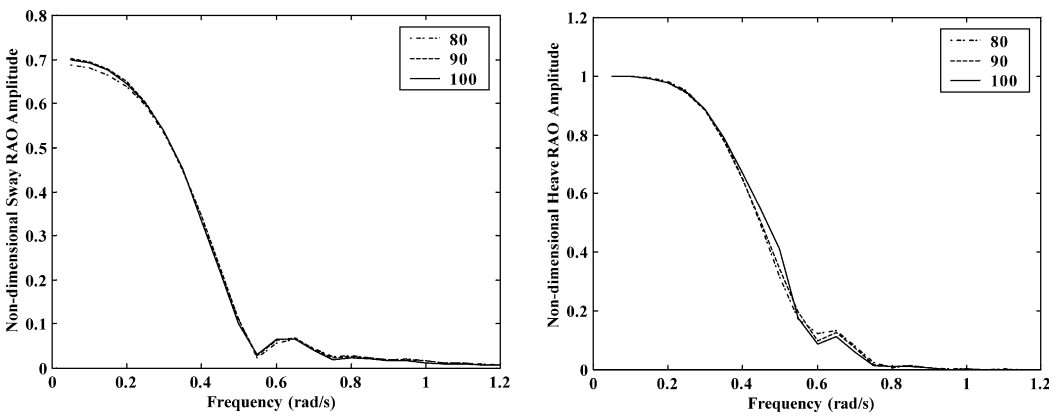

Fig. 1. (a) Sway and (b) Heave RAO amplitude for 100, 90 and 80% loading conditions.

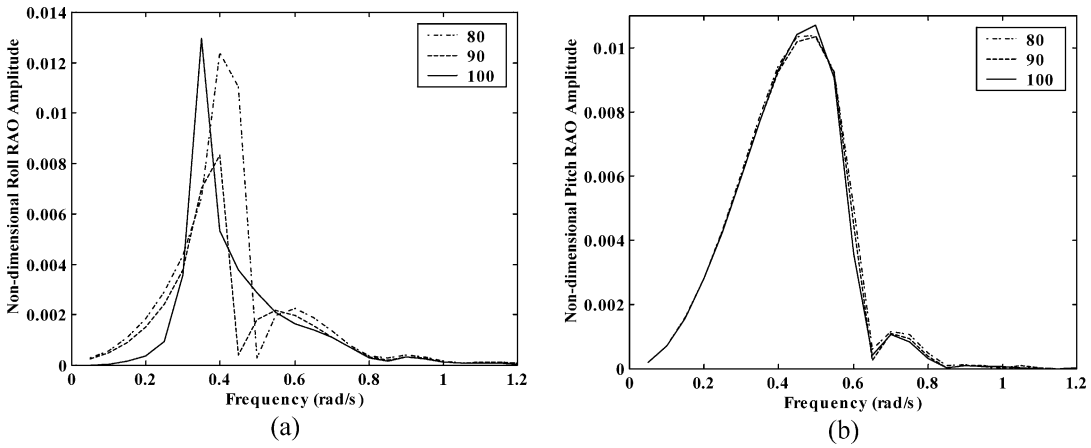

Fig. 2. (a) Roll and (b) Pitch RAO amplitude for 100, 90 and 80% loading conditions.

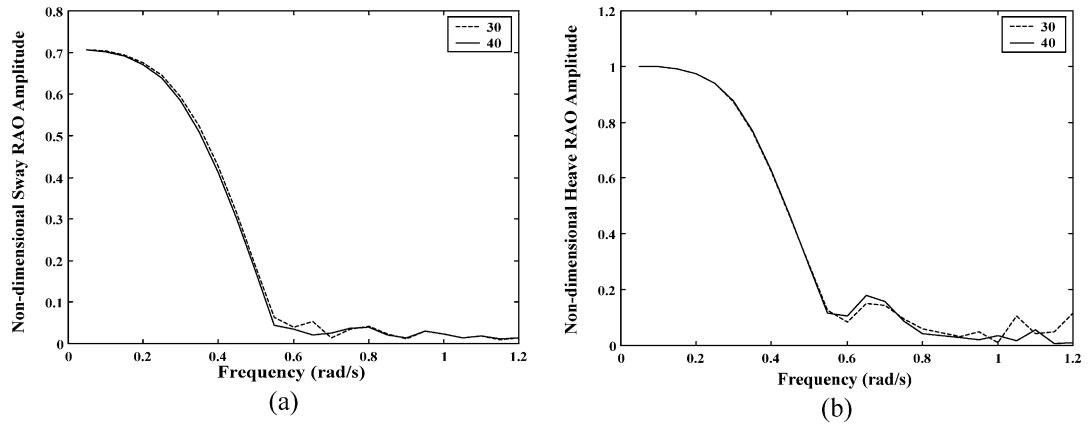

Fig. 3. (a) Sway and (b) Heave RAO amplitude for 40 and 30% loading conditions.

sensitivity to loading conditions as illustrated by Figs. 1 and 5.

Roll RAO is an odd function of the incidence angle, and it takes into account if waves come from port or starboard. This information is not contained in pitch and heave motions, since the corresponding RAO's are even functions of incidence angle. Since sway RAO is also an odd function and taking into account the considerations above, it can advantageously replace roll in the estimation procedure.

The estimation method was then applied to sway, heave and pitch motions. However, even in this case, some sensitivity to loading conditions is expected, since RAO's phase plots present a significant variation specially for heave and pitch motions, as can be seen in Figs. 6 and 7.

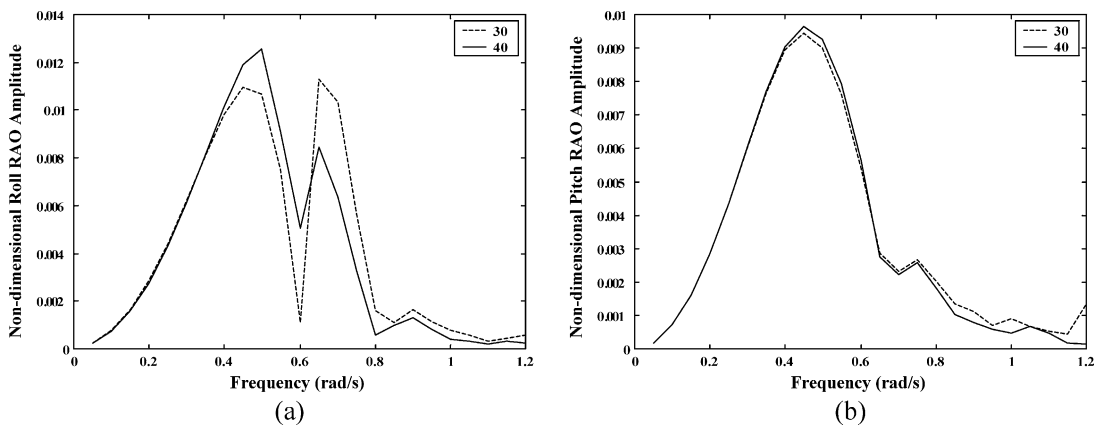

Fig. 4. (a) Roll and (b) Pitch RAO amplitude for 40 and 30% loading conditions

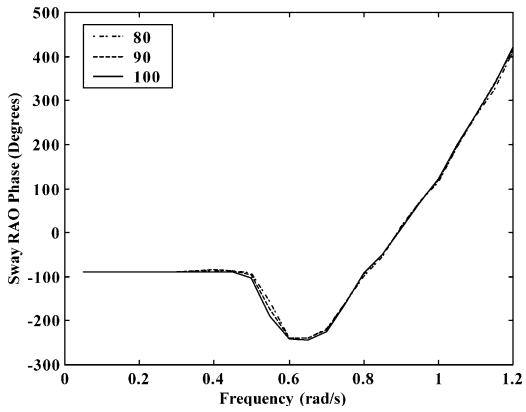

Fig. 5. Phase of sway RAO for 80, 90 and 100% loading conditions.

The influence of such variations in the final estimated spectrum is analysed in the next section.

4. Numerical tests

As a first test of the methodology, accuracy and robustness, a series of numerical simulations was performed, using as example the VLCC Vidal de Negreiros in a variety of environmental conditions.

The first set of trials was carried out in non-real conditions, supposing that the RAO's are perfectly known. This was done in order to evaluate the numerical performance and mathematical behavior of the methods. The ship is considered fully loaded; so, 100% RAO's are used both to generate ship motions ("real" model) (by means of Eq. (1)) and in the algorithm ('ideal' model).

As it should be expected, the Parametric Method generated good estimates and converged to the real spectrum with good accuracy.

In order to evaluate the sensitivity of the methods to some degree of uncertainty in RAO's, the second set of trials used different loading conditions in the generation of ship motions ("real" model) and in the estimation algorithm ("ideal" model), emulating an uncertainty in the RAO's.

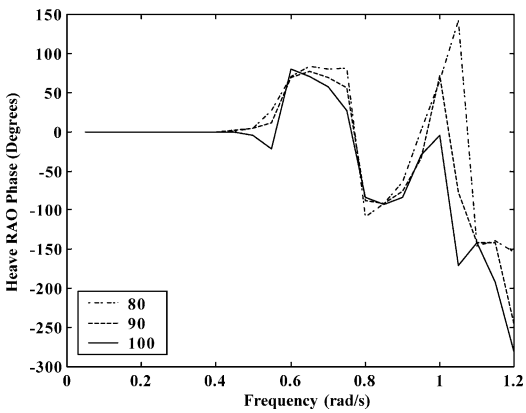

Fig. 6. Phase of heave RAO for 80, 90 and 100% loading conditions.

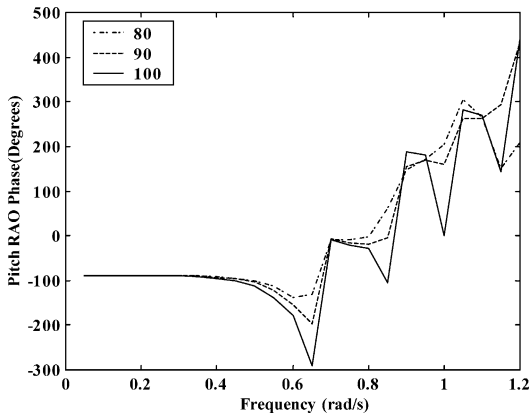

Fig. 7. Phase of pitch RAO for 80, 90 and 100% loading conditions.

Two loading conditions were considered in these analyses:

- Fully loaded condition: the 90% loaded ship RAO's were used in the generation of motions ('real' model) and the 100% loaded ship RAO's were used in the estimation method ("ideal" model).
- Ballasted condition: the 30% loaded ship RAO's were used in the generation of motions ("real" model) and the 40% loaded ship RAO's were used in the estimation method ('ideal' model).

Three types of numerical tests were carried out. In section A, unimodal sea states with peak pseriod between 7 and 20 s were considered. This analysis was used to estimate the cut-off frequency of the method both for the full and ballasted conditions of the VLCC tanker. Section B and C presents the application of real Campos Basin DWS, considering 1 and 100-year unimodal in section B and bimodal cases in section C.

4.1. Analysis of unimodal spectrum with peak periods between 7 and 20 s

Initially, a unimodal sea-state with significant wave height $Hs = 1$ m and peak period T_p between 7 and 20 s was considered. Three possible wave-ship headings were assumed for motion generation, namely 90, 135 and 180°, as shown by Fig. 8. A large value for spreading coefficient $s_1 = 60$ was used in order to emulate an unidirectional wave pattern. The incident wave spectrum has $\lambda_1 = 1$.

Fig. 9 presents the results of the Parametric Method for the fully loaded condition. The maximum estimation errors obtained for the three heading angles are shown as function of peak period. It can be seen that for periods higher than 11 s, the maximum errors for height, period and direction are smaller than 7.5%, 2.5% and 1.5°, respectively.

The loss of accuracy for smaller wave periods can be explained by the fact that the ship does not respond to such waves, as already said. Indeed, considering for instance a beam-sea incidence of a 2 m height wave, Table 2 shows

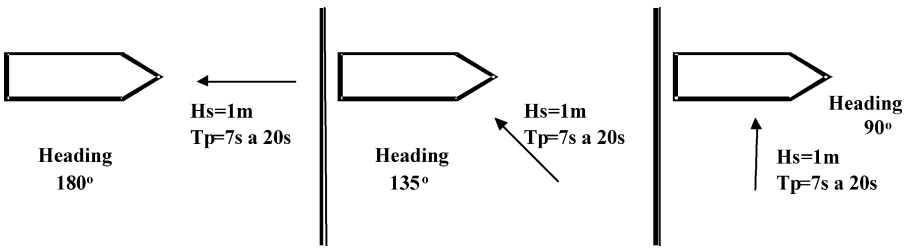

Fig. 8. Wave-ship headings considered in the analysis.

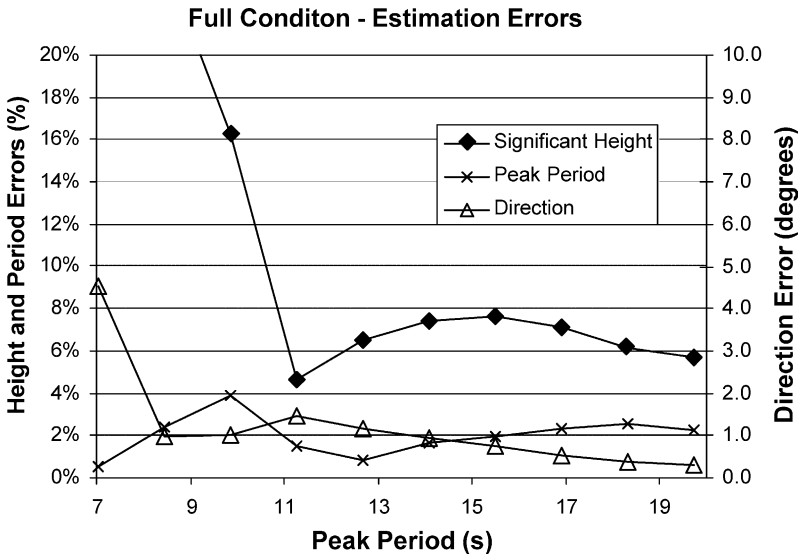

Fig. 9. Maximum estimation errors for unimodal waves with $Hs = 1$ m and $T_p = 7$ s to 20s-Fully loaded condition.

the maximum amplitude of ship motions for $T_p = 8.5$ s and $> T_p = 17$ s. It can be seen that ship motion is extremely reduced for wave periods below 6 s.

The analysis above was performed to define a 'cut-off' frequency of the method when applied to the fully loaded VLCC. As a consequence, it was decided that estimated spectra with estimated peak period bellow 11 s should be discarded, since they may present large relative errors. For periods higher than 11 s, the estimated spreading coefficient varied between 57 and 74.

The results for the ballasted condition are presented in Fig. 10. For peak periods above 10 s, the maximum errors are bounded by 9, 3.5% and 1.3°, respectively. In this case, the errors are smaller than in the full loaded condition, and the estimates remain satisfactory for a slightly broader range of wave periods ($T_p > 10$ s). This fact was expected since the ballasted ship inertia is smaller than for the full loaded condition, and it responds more intensely to waves. In the ballasted case, the estimated spreading coefficient varied between 43 and 63.

As already said, accurate estimation of mean drift forces and moment plays an important role in modern feed forward DP Systems. Such forces are evaluated by a simple spectral crossing, given by:

$$F_{i\mathrm{MD}} = \int_0^{\infty} \int_0^{2\pi} S(\omega, \theta).D_j(\omega, \theta).d\theta.d\omega \tag{5}$$

where $i = 1$ for surge force, $i = 2$ for sway force, $i = 6$ for yaw moment and D is the drift coefficient, obtained by potential wave theory and numerical integration along ship hull.

For the sake of illustration, the mean drift forces were evaluated using both the real and the estimated spectra. The relative errors are presented in Fig. 11 (fully loaded condition) and Fig. 12 (ballasted condition). A 180° incidence for surge force, 90° incidence for sway force and 135° incidence for yaw moment were considered. The errors can be considered satisfactory (smaller than 20%) for wave

Table 2
Maximum amplitude of ship motions

	$T_p = 8.5$ s	$T_p = 17$ s
Sway	0.3 m	1.1 m
Heave	0.5 m	1.7 m
Pitch	0.3°	0.6°

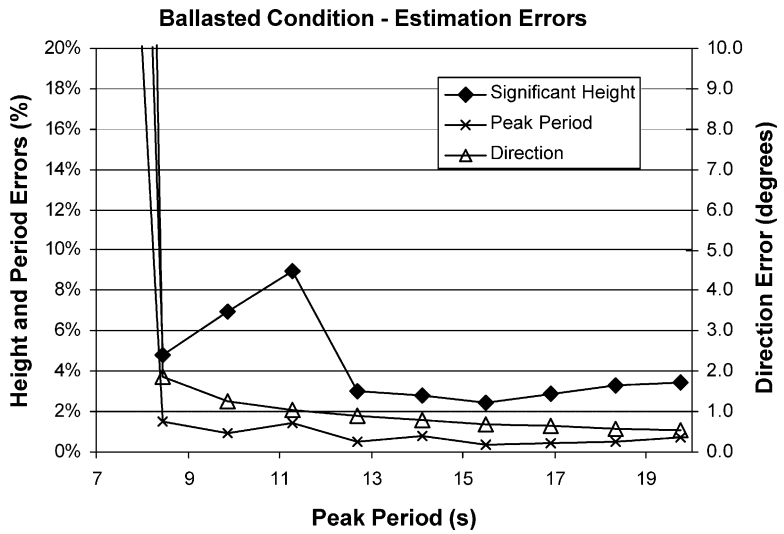

Fig. 10. Maximum estimation errors for unimodal waves with $Hs = 1$ m and $T_p = 7-20$ s—ballasted condition.

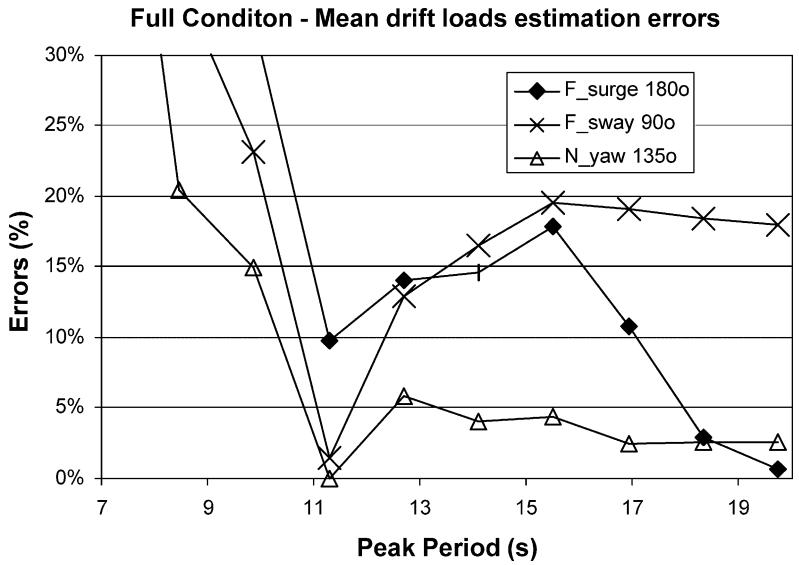

Fig. 11. Estimation errors for mean drift forces, with $Hs = 1$ m and $T_p = 5-20$ s—Fully loaded condition.

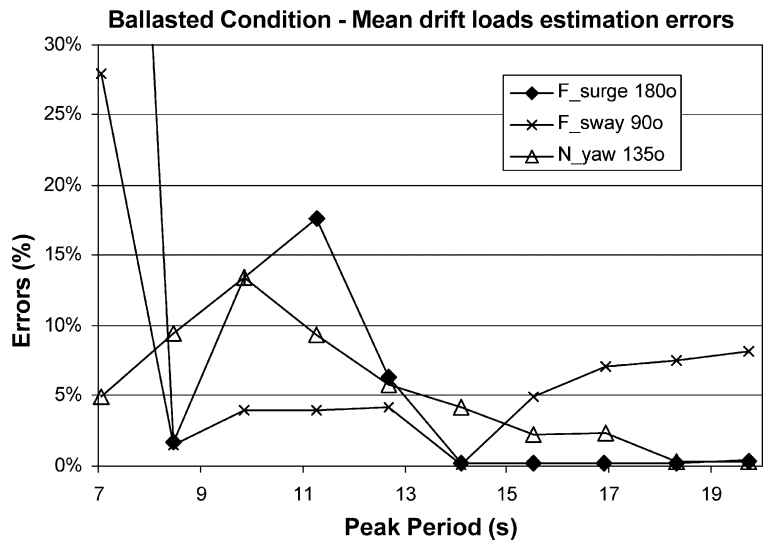

Fig. 12. Estimation errors for mean drift forces, with $Hs = 1$ m and $T_p = 5-20$ s—Ballasted condition.

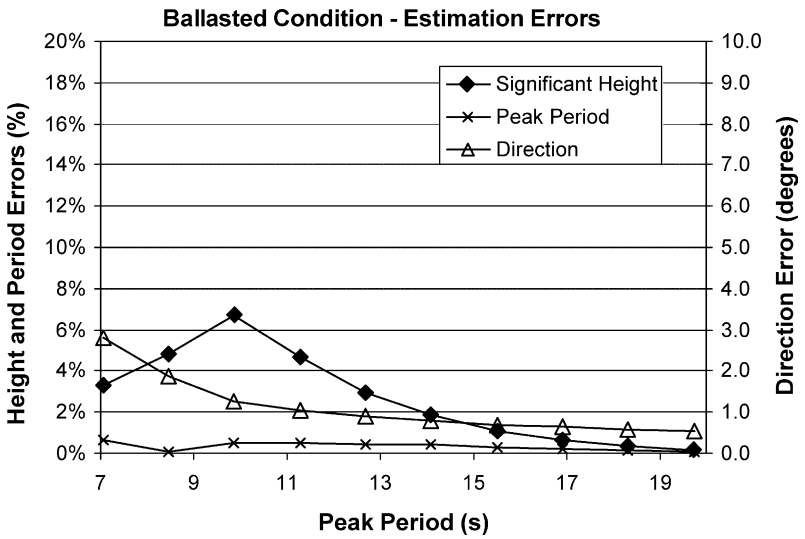

Fig. 13. Maximum estimation errors for unimodal waves with $Hs = 1$ m and $T_p = 7$–s–BGL1 barge.

periods higher than the cut-off period. This level of accuracy is adequate for control purposes, since modern controllers are robust in the sense that they satisfy performance requirements under bounded modeling and estimation errors. An example of integration between the proposed Parametric Estimation Method and a robust controller is presented in Ref. [12].

Notice that the errors are larger in the forces than in the estimated spectrum parameters. This can be easily understood if we observe that the significant wave height had the largest estimation errors in almost all tests and the forces are proportional to the square of it (see Eqs. (4) and (5)).

Extreme wave conditions are normally characterized by larger periods, as will be exposed in section B. So, even with the loss of accuracy of the present method for short period waves, it will be able to be used in extreme wave feedforwad control.

The method was also applied to BGL-1, a pipe-laying barge that operates in Brazilian waters. The barge length is 121.9 m and its mass is 17177 ton. A 10% error in draft is also assumed for the application of the method. Fig. 13 presents estimation errors for 135° incidence angle. Indeed, errors are smaller than those obtained for the FPSO, confirming the fact that the method is better for smaller ships since the ship motions have larger amplitudes. In this case, the minimum peak period that can be estimated is smaller than 7 s.

A Bayesian Method was also implemented, based on Ref. [7,8]. Extensive numerical simulations were carried out to adjust all parameters involved in such methodology in order to obtain the best possible results. Fig. 14 presents the results for the fully loaded condition. It can be seen that such method is strongly sensitive to RAO's uncertainties, leading to estimation errors much higher than those obtained with the Parametric Method. The results obtained for the ballasted condition are slightly better, but they still present unacceptable errors. Although the Bayesian Method is much faster than the Parametric one, since it requires only

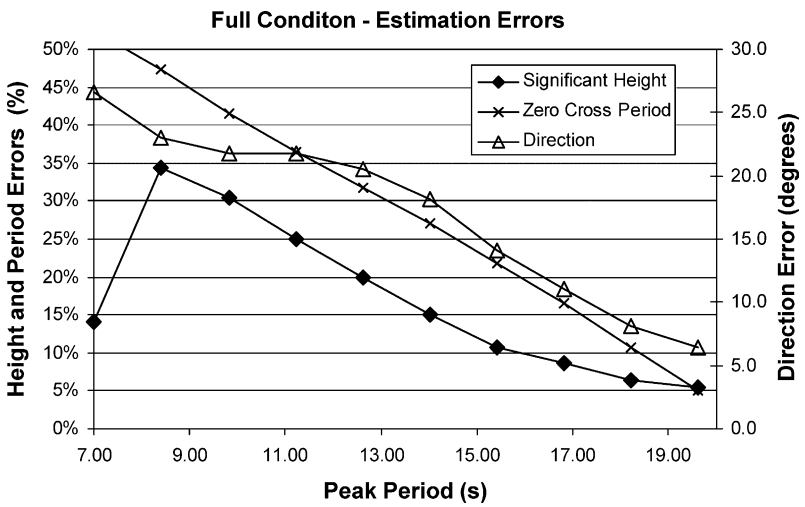

Fig. 14. Maximum estimation errors for unimodal waves with $Hs = 1$ m and $T_p = 5$–20 s using the Bayesian Method—Fully loaded condition.

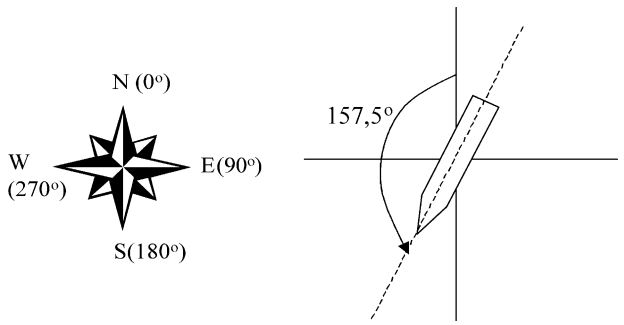

Fig. 15. Ship heading considered in the 1-year and 100-year wave analysis.

a quadratic programming algorithm instead of a generic non-linear minimization one, the results are poor.

All other numerical tests performed confirmed that the accuracy of the Parametric Method is higher than the one presented by the Bayesian Method. So, only the results of the Parametric Method are presented in the following.

4.2. B. Application to extreme 1-year and 100-year unimodal waves in Campos Basin

The previous analysis was used to estimate the cut-off frequency of the method both for the full and ballasted conditions of the VLCC tanker.

The method was then applied to 1-year and 100-year waves in Campos Basin. The ship heading considered in the present analysis is 157.5° with respect to North direction, as shown in Fig. 15.

The results obtained for 1-year waves are shown in Table 3. It can be seen that for the full load condition, the error is smaller than 7% for wave height, 1.2% for peak period and 1.9° for mean direction. Even for W and NW waves, which have peak periods smaller than the estimated cut-off period of 11 s, the errors are acceptable.

For ballasted condition, the estimation errors are smaller than 7, 2.3% and 1.8° for height, period and mean direction, respectively.

The SE 1-year spectrum is represented in Fig. 16. In this wave spectrum contour plot, the circles correspond to the indicated frequencies of 0.4, 0.8 and 1.2 rad/s. It can be clearly seen that the overall shape and directional spreading of the estimated spectra are quite similar to the real one, both for the fully loaded and ballasted conditions.

As the method presented good results when applied to 1-year waves, even better results were expected in the case of 100-year waves, since the significant height and peak period are higher, giving rise to higher ship motions. Indeed, the results for 100-year waves are presented in Table 4, where it can be seen that the maximum errors for the full loaded condition are of 4, 1% and 1.6° for height, period and direction, respectively. As expected, these errors are smaller than those obtained for the 1-year wave estimation. Furthermore, for the ballasted condition the errors are smaller than 2%, 0.5% and 0.7° for height, period and direction, respectively.

In the analyses presented in Tables 3 and 4, $s_1 = 60$ and $\lambda_1 = 1$ were used again. The estimated spreading coefficient varied between 40 and 70.

It must be emphasized that in all the cases exposed above, the Parametric Method returned the full vector of parameters $x = [\omega_{m1}\ Hs_1 s_1\, \theta_{m1}\, \omega_{m2} Hs_2 s_2\, \theta_{m2}]^T$. Since the real spectrum in these cases is unimodal, one of the estimated significant heights was indeed negligible, and the corresponding peak was disregarded by a post-processor algorithm.

4.3. Bimodal spectra

Finally, the method was applied to typical bimodal spectra observed in Campos Basin. An exhaustive analysis was carried out, considering the highest probability sea-states in the region, using the data recorded during 5 years by a directional buoy operated by Petrobras [13].

Since bimodal sea states presented in this section are not extreme, the present analysis would not be applied in a DP feedforwad wave compensation technique. The only objective here is to clarify and exemplify the estimation method.

Table 5 presents the results for two different cases, summarizing all the analyses done. The ship is headed to Southeast direction.

Table 3
Annual waves in Campos Basin

	Real spectrum parameters			Estimated parameters (loaded condition)			Estimated parameters (ballasted condition)		
	Hs (m)	T_p (s)	θm (^{0})	*Hs* (m)	T_p (s)	θm (^{0})	*Hs*(m)	T_p (s)	θm (^{0})
N	4.2	12.4	0.0	4.1	12.5	0.7	4.1	12.4	-0.7
NE	3.9	12.0	45.0	3.7	12.1	45.0	3.9	12.1	46.8
E	3.7	11.7	90.0	3.7	11.7	88.1	3.6	11.7	91.0
SE	4.5	12.7	135.0	4.2	12.8	136.2	4.4	12.7	134.8
S	5.1	13.4	180.0	5.0	13.4	179.6	5.0	13.4	178.9
SW	5.7	14.1	225.0	5.3	14.2	225.0	5.7	14.1	225.0
W	3.0	10.7	270.0	3.1	10.7	269.1	2.8	10.7	271.2
NW	3.0	10.7	315.0	3.1	10.4	313.6	2.9	10.7	315.1

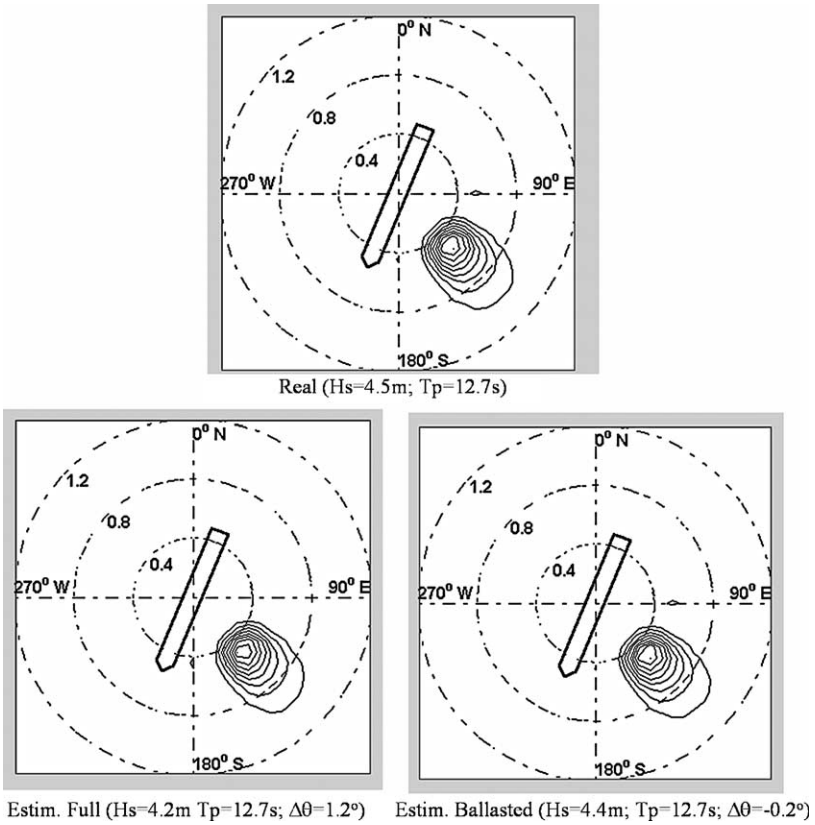

Fig. 16. SE 1-year spectrum.

Table 4
Centenary waves in Campos Basin

	Real spectrum parameters			Estimated parameters (loaded condition)			Estimated parameters (ballasted condition)		
	Hs (m)	T_p (s)	θm (^{0})	*Hs* (m)	T_p (s)	θm (^{0})	*Hs* (m)	T_p (s)	θm (^{0})
N	6.3	14.6	0.0	6.2	14.6	−1.2	6.2	14.6	−0.6
NE	5.4	13.8	45.0	5.3	13.8	46.4	5.3	13.8	45.7
E	4.7	12.9	90.0	4.6	13.0	91.3	4.7	12.9	90.0
SE	6.7	15.1	135.0	6.6	15.2	135.8	6.7	15.1	134.7
S	7.0	15.3	180.0	6.9	15.3	180.0	7.0	15.3	179.5
SW	7.8	16.2	225.0	7.8	16.2	224.2	7.7	16.2	225.4
W	4.9	13.2	270.0	4.9	13.2	269.5	4.8	13.2	270.7
NW	4.9	13.2	315.0	4.7	13.4	313.4	4.8	13.2	315.6

Table 5
Bimodal spectra estimation

		Peak 1					Peak 2				
Cond		*Hs*1	T_p1	λ1	*s*1	θ1	Hs_2	T_{p2}	λ2	*s*2	θ2
A	Real	1.76	12.05	1.5	17.10	182.20	1.08	5.93	1.2	23.70	98.30
	Full	2.02	11.50	1.0(*)	19.30	180.30	–	–	–	–	–
	Ballasted	1.67	12.09	1.0(*)	17.20	180.80	–	–	–	–	–
B	Real	1.52	6.12	1.5	19.90	186.30	0.64	11.64	1.2	23.50	140.50
	Full	–	–	–	–	–	0.75	10.94	1.0(*)	13.89	141.72
	Ballasted	–	–	–	–	–	0.69	10.99	1.0(*)	8.56	141.16

(*) This parameter was not estimated. It is supposed $\lambda_i = 1$, as already explained.

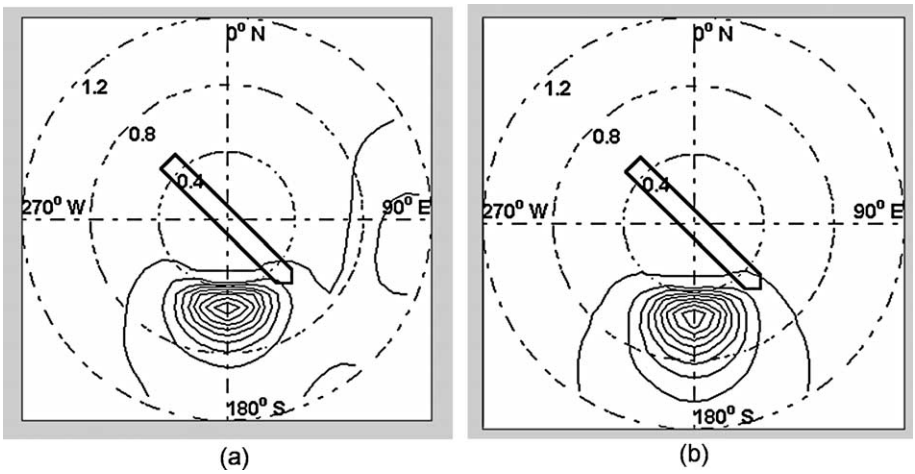

Fig. 17. Bimodal spectrum in condition A. (a) Real spectrum (b) Estimated spectrum in full loaded condition.

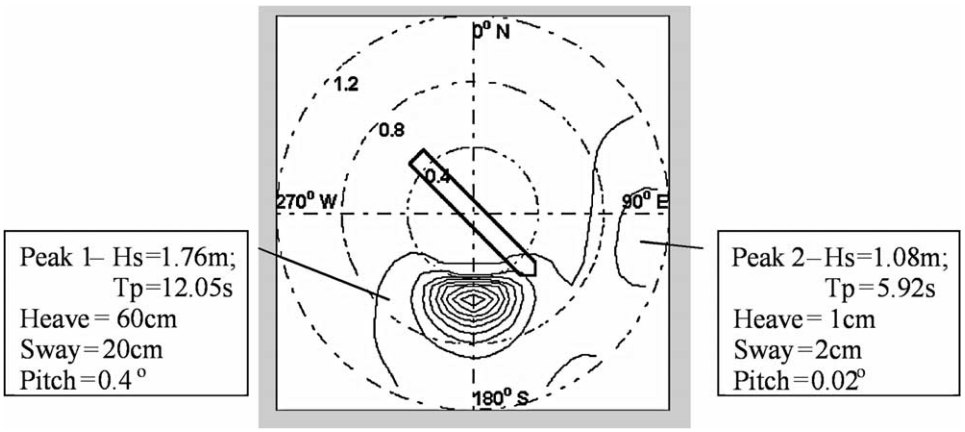

Fig. 18. Maximum ship motions for both peaks (Cond. A—full loaded ship).

Table 6
Bimodal spectra estimation

Cond		Peak 1					Peak 2				
		Hs_1	T_{p1}	$\lambda 1$	$s1$	$\theta 1$	Hs_2	T_{p2}	$\lambda 2$	$s2$	$\theta 2$
C	Real	1.76	12.05	1.5	17.10	182.2	1.08	12.05	1.2	23.70	98.3
	Full	2.18	11.45	1.0(*)	13.60	175.2	0.96	12.16	1.0(*)	13.90	97.8
	Ballasted	2.02	11.68	1.0(*)	14.32	180.3	1.02	12.08	1.0(*)	20.25	97.3

(*) this parameter was not estimated. It is supposed $\lambda_i = 1$, as already explained.

The first condition in Table 5 (Cond.A) corresponds to the case where the first peak (the peak with the highest significant height) has a peak period of 12.05 s and the waves come from Southern direction. The second peak has a higher frequency, with 5.93 s peak period. As expected, the second peak could not be recovered neither in loaded nor in ballasted condition, since its peak period is smaller than the cut-off period previously determined (10 s for ballasted ship and 11 s for loaded one). The first peak, however, was estimated with an error bellow 14% for height, 5% period and 2° for direction. It can be seen that spreading estimation presents higher errors which is

Table 7
VLCC characteristics in 3 loading conditions considered in experiments

Properties	Full loaded	Intermediate	Ballasted
Mass (M)	302028 ton	198944 ton	115838 ton
Draft (T)	21.0 m	14.7 m	9.0 m
Roll radius of gyration	16.83 m	16.92 m	23.22 m
Pitch radius of gyration	86.31 m	82.43 m	90.54 m
Yaw radius of gyration	80.00 m	80.00 m	80.00 m

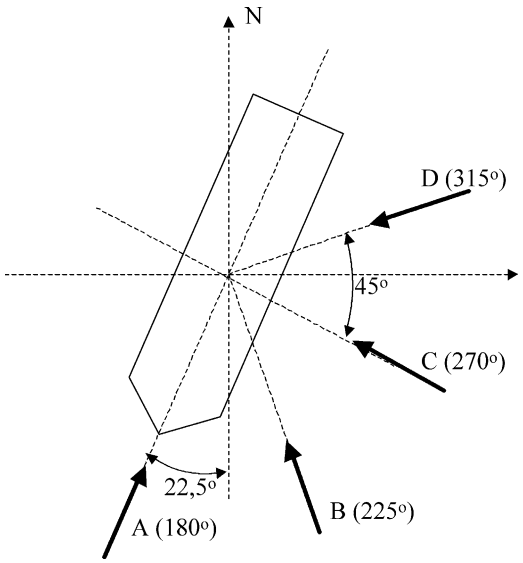

Fig. 19. Wave incidence directions of experiments (angles with respect to longitudinal axis of the ship).

expected since the ship motions are less dependent on it. Once again, for all the spectrum parameters estimation results for the ballasted case are better than for the full loaded ship. The method evaluated the full estimated parameter vector $x = [\omega_{m1}\ Hs_1\ s_1\ \theta_{m1}\ \omega_{m2}\ Hs_2\ s_2\ \theta_{m2}]^T$ Since the second estimated frequency ω_{m2} was greater than the cut-off frequency previously obtained, the post-processor algorithm disregarded the corresponding peak.

Furthermore, even in the presence of an incident spectrum with $\lambda_i \neq 1$, the estimation accuracy of Hs_i, ω_{mi} and θ_{mi} is good.

This type of spectrum, in which the peak with highest significant height has the peak period higher than 10 s, corresponds to 36% of all the registered spectra in the analysis carried out in Campos Basin [13].

The second class of spectra is represented by Cond.B in Table 5, in which the second peak (namely, the peak with the lowest significant height) presents the peak period greater than 10 s (in this case, 11.64 s). It can be seen that

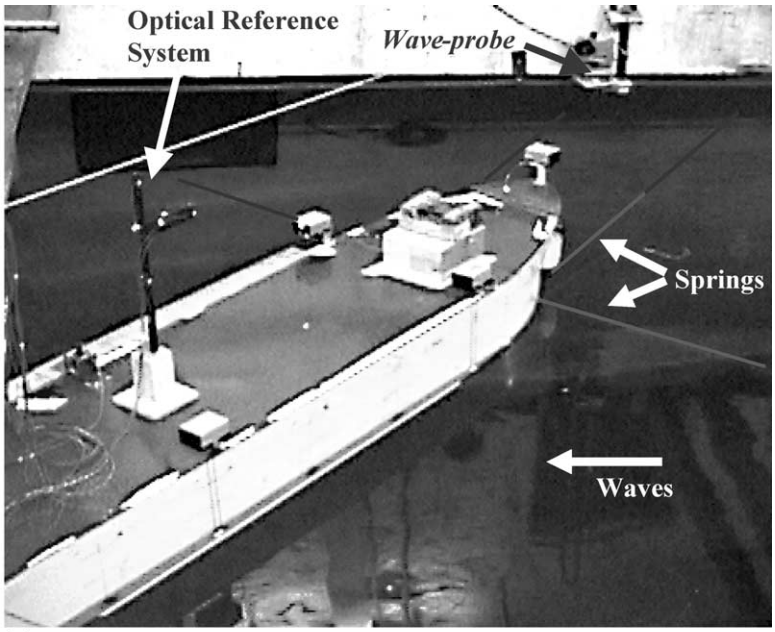

(a)

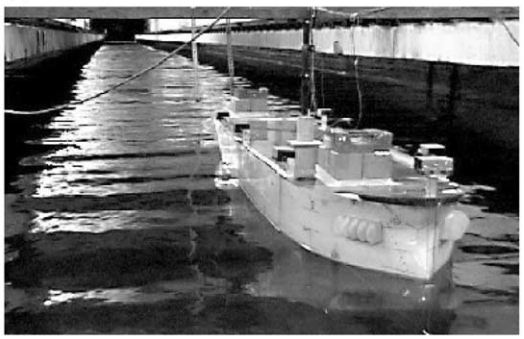

(b)

Fig. 20. (a) Experimental set-up during a trial with wave incidence B (b) Trial with wave incidence A.

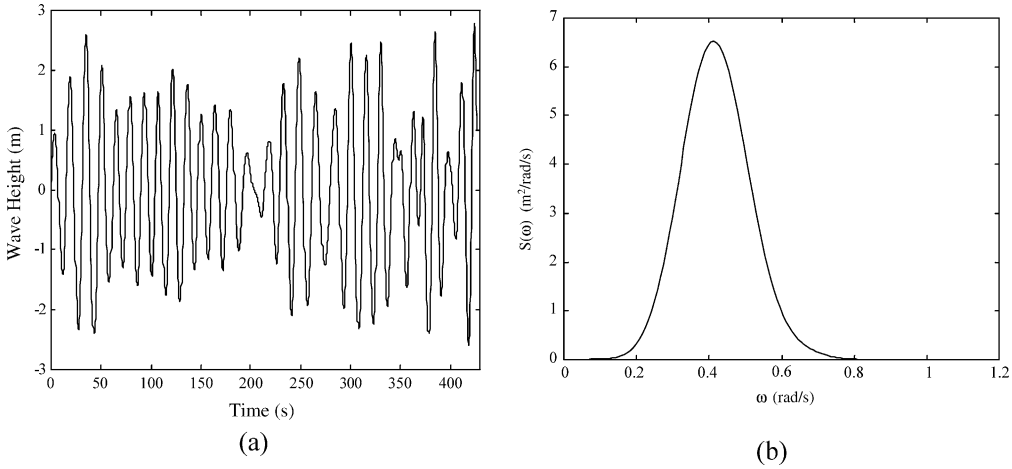

Fig. 21. (a) Wave-height time series (b) Wave power spectrum (both plots were transferred to real scale).

the second peak was recovered with errors smaller than 17% for height, 6% for period and 1.2° for direction. The first peak could not be estimated, since its peak period is smaller than the cut-off period both in ballasted and full loaded conditions. This class of spectrum corresponds to 16% of the registered cases in Ref. [13].

As expected, the 48% remaining registered spectrum presented both peaks with periods smaller than 10 s. Consequently any peak of this class of spectra could not be recovered by the method neither in full loaded nor in ballasted condition. Fortunately these sea states do not induce harmful motions in the system.

The first spectrum (Cond.A) is represented in Fig. 17(a), with the ship headed to Southeast direction. The first peak comes from South (182.2°) and the second peak comes from East (98.3°). The estimated spectrum in the full-loaded condition is shown in Fig. 17(b). It can be seen that the first peak has been recovered with a slight deformation in the shape mainly for high-frequency components. As already discussed, the second peak has not been recovered.

In order to exemplify the relative importance of the peaks, the maximum amplitude of each motion is evaluated for the previous case, assuming individual incidence of the peaks. The results are presented in Fig. 18 where it can be seen that the second peak induces small motions in the ship indeed.

An artificial case (Condition C) was also analysed, aiming to determine the ability of the method in estimating bimodal spectra in which both peaks have average zero-crossing periods greater than 8 s. Indeed, Table 6 shows that the both peaks are estimated with errors smaller than 24% for wave height, 5% for period and 7° for direction. Again, it can be seen that the spreading parameter estimation presents higher errors, which is expected since the motions of the ship are less dependent on them.

5. Experimental results

The Parametric Method was applied to model-scale experiments carried out in IPT towing tank. A 1:90 reduced model of VLCC Vidal de Negreiros was used. Three loading conditions were considered whose main characteristics transposed to real scale are given in Table 7.

The ship was moored by 8 linear springs, representing a spread mooring system with differential compliance (DICAS). The initial heading of the model was 202,5° with respect to the Northern direction.

Experiments were conducted considering only unimodal and unidirectional sea states. Fig. 19 shows the four wave incidence directions considered.

An optical reference system was used to measure all ship motions. Wave height were measured by a capacitive wave probe installed close to the model (Fig. 20).

All trials lasted approximately 47 s (equivalent to 7.5 min in real scale), and the measurements were performed with a sampling rate of 51 Hz (5,4 Hz in real scale). Cross spectra functions of ship motions were evaluated by Welch Method (Welch, 1967), with 4096-sample FFT, 256-sample Hanning windowing with 128-sample overlap.

In the present experiment, ship yaw was almost constant, with variations smaller than 2° due to the stiff springs used

Table 8
1, 10 and 100-year extreme wave conditions

Incidence	1-year		10-year		100-year	
	Hs	T_p	*Hs*	T_p	*Hs*	T_p
A	5.7 m	13.7 s	6.9 m	14.6 s	7.8 m	15.3 s
B	5.1 m	13.2 s	6.1 m	14.0 s	7.0 m	14.7 s
C	4.5 m	10.3 s	5.5 m	10.8 s	6.7 m	11.3 s
D	3.9 m	8.5 s	4.7 m	9.0 s	5.4 m	9.4 s

Table 9
Parametric method results—estimation errors in parenthesis

Cond.	Incidence	Trial	*Hs* real (m)	T_p real (s)	*Hs* est (m)	T_p est (s)	Dir. est
Full loaded	A (180°)	1	6.4	14.6	7.3 (15%)	13.0(−10%)	180.2° (0°)
		2	7.0	14.8	7.2 (3%)	13.9(−6%)	180.2° (0°)
		3	7.8	13.3	8.5 (9%)	12.6(−5%)	180.2° (0°)
		4	9.0	14.5	9.8 (8%)	13.9(−4%)	180.2° (0°)
	B (225°)	1	4.9	15.2	6.0 (22%)	14.8 (−2%)	217.4° (−8°)
		2	6.1	12.9	7.7 (26%)	13.2 (3%)	225.4° (0°)
		3	9.1	12.7	9.0 (−1%)	13.6 (7%)	214.4°(−11°)
		4	7.3	14.3	8.8 (21%)	14.1 (−1%)	214.7°(−10°)
	C (270°)	1	5.3	10.8	4.3 (−18%)	11.0 (1%)	269.1° (1°)
		2	5.3	10.9	4.2 (−19%)	11.3 (4.8%)	269.1° (1°)
		3	6.8	10.9	5.2 (−24%)	11.5 (5%)	269.3° (1°)
		4	7.8	11.0	5.8 (−25%)	11.5 (5%)	269.6° (0°)
	D (315°)	1	4.3	10.0	5.4 (26%)	9.8 (−2%)	337.0° (22°)
		2	4.9	9.5	6.7 (−5%)	9.7 (2%)	339.0° (24°)
		3	5.7	10.1	7.5 (31%)	9.4 (−7%)	358.1° (43°)
		4	6.0	10.2	5.0 (−18%)	10.2 (0%)	351.2° (36°)
Intermediate	A (180°)	1	6.6	14.9	6.4 (−4%)	13.4(−10%)	180.0° (0°)
		2	6.8	15.2	6.8 (0%)	13.7(−10%)	180.0° (0°)
		3	8.2	13.6	9.0 (10%)	12.7 (−6%)	180.0° (0°)
		4	9.4	14.6	9.6 (2%)	13.5 (−7%)	180.0° (0°)
	B (225°)	1	5.0	15.2	5.8 (15%)	14.6 (−3%)	221.7° (−3°)
		2	6.3	13.3	6.6 (4%)	13.2 (−1%)	217.8° (−7°)
		3	8.6	13.1	8.4 (−2%)	13.5 (3%)	222.5° (−3°)
		4	7.7	14.0	8.3 (8%)	14.0 (0%)	222.4° (−3°)
	C (270°)	1	4.8	10.8	5.2 (8%)	11.3 (4%)	268.8° (−1°)
		2	6.2	10.9	6.0 (−4%)	12.6 (16%)	269.4° (−1°)
		3	7.8	10.3	6.5 (−16%)	11.8 (15%)	269.3° (−1°)
		4	6.6	10.7	6.5 (−1%)	11.3 (6%)	269.1° (−1°)
	D (315°)	1	4.3	9.8	5.9 (36%)	9.8 (0%)	353.8° (39°)
		2	5.3	9.6	6.2 (18%)	9.4 (−2%)	344.5° (30°)
		3	5.1	10.1	8.7 (70%)	9.6 (−5%)	354.7° (40°)
		4	5.9	10.2	6.7 (14%)	9.9 (−3%)	354.9° (40°)
Ballasted	A (180°)	1	6.7	14.6	6.7 (0%)	13.5 (−8%)	180.0° (0°)
		2	7.1	14.3	6.9 (−4%)	14.1 (−2%)	180.0° (0°)
		3	8.4	14.1	8.4 (0%)	13.2 (−6%)	180.0° (0°)
		4	9.3	14.9	10.2 (9%)	13.4(−10%)	180.0° (0°)
	B (225°)	1	4.9	15.2	5.9 (20%)	14.3 (−6%)	224.6° (0°)
		2	6.1	13.3	7.0 (15%)	12.9 (−3%)	220.0 ° (−5°)
		3	8.4	13.6	8.7 (4%)	13.3 (−2%)	224.0 ° (−1°)
		4	7.5	14.3	8.3 (11%)	13.9 (−3%)	225.7 ° (1°)
	C (270°)	1	4.1	10.8	5.1 (24%)	11.4 (5%)	269.5° (−1°)
		2	6.2	11.2	6.2 (0%)	12.5 (12%)	269.7° (0°)
		3	6.2	10.3	7.5 (20%)	11.3 (11%)	269.7° (0°)
		4	6.1	10.7	7.0 (15%)	11.4 (7%)	269.6° (0°)
	D (315°)	1	4.4	10.1	7.7 (74%)	9.5 (−6%)	351.0° (36°)
		2	4.8	9.7	8.7 (80%)	9.2 (−5%)	337.7° (23°)
		3	5.3	10.0	10.1 (0%)	9.5 (−5%)	358.2° (43°)
		4	5.8	10.1	8.3 (42%)	9.5 (−6%)	350.8° (36°)

in the mooring system. However, real applications can present higher yaw variations, which changes the incident wave direction with respect to the ship and influences the estimate. Such problem isn't addressed in the present work, but it was treated by Ref. [14], in which the authors performed the average of spectral blocks of the Welch method for each heading separately.

The real incident wave spectrum was obtained by means of wave-height time series measured by wave-probe. It was used for confrontation with spectrum estimated by Parametric Method using only ship motions measurements. For example, Fig. 21(a) shows wave-height time series for an incidence B experiment, and Fig. 21(b) contains the respective wave power spectrum.

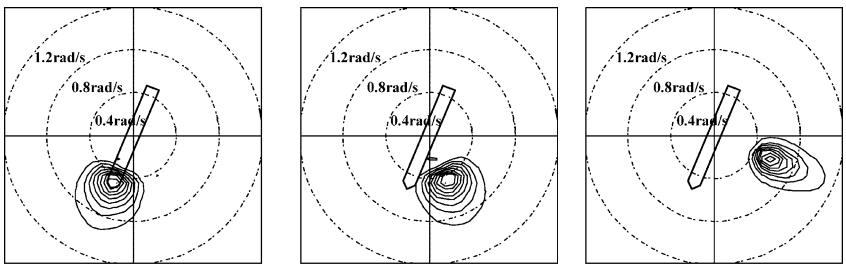

Fig. 22. Examples of estimated spectra for 3 incidences.

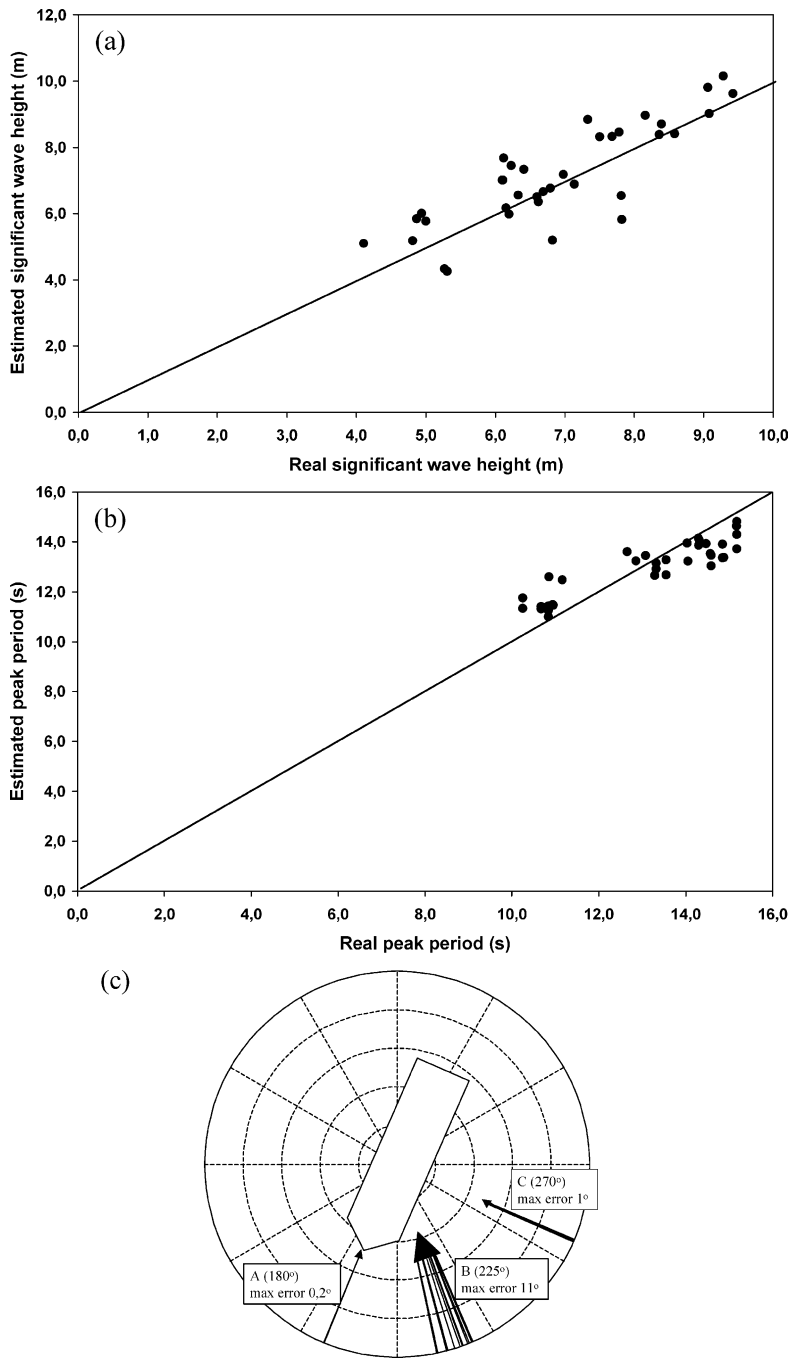

Fig. 23. Parametric method results (a) Significant wave height; (b) Peak period; (c) Direction.

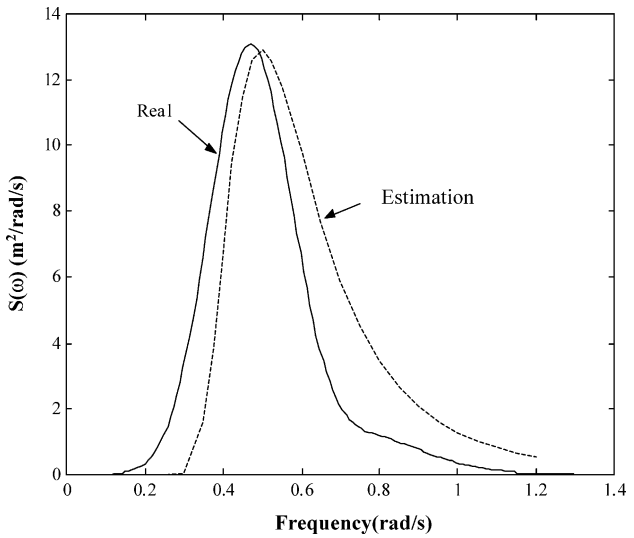

Fig. 24. Estimated and measured wave power spectra. Full loaded condition, incidence A, trial 3.

For unimodal waves, the significant wave height is related to wave power spectrum by:

$$H_S = 4\sqrt{\int_0^\infty S(\omega)\mathrm{d}\omega}$$

The peak period T_p is the period with maximum power spectrum, and it can be shown to correspond to the modal frequency previously defined ($T_\mathrm{p} = 2\pi/\omega_m$). These parameters ($Hs$ and T_p) were evaluated for each experiment, using the wave power spectrum obtained by wave-height time series. Such parameters were used for comparison with the estimates obtained by the Parametric Method. 1, 10 and 100-year extreme wave conditions were used for each incidence usually observed in the Campos Basin. The significant wave height and peak period for these cases are given in Table 8.

The results of the Parametric Method are presented in Table 9. The experiments with estimated peak period smaller than 11 s (full loaded) and 10 s (ballasted and intermediate loading) are shaded (all experiments with incidence D). These results must be discarded since the numerical analyses presented in section 4 showed that these wave conditions cannot be estimated by the Parametric Method.[2] Indeed, large estimation errors were obtained for these experiments, reaching 80% for significant height and 70° for mean direction. However, peak period is accurately estimated, with errors smaller than 7%. Hence a comparison of the estimated peak period with its theoretically predicted range permits the analyst to decide whether the estimates of the remaining parameters are trustable or not. For the full loaded case in wave incidence C, the real peak period is close to the theoretical estimation limit of 11 s and the estimates lie in the range between 11.0 and 11.5 s, just above the limit. In these cases, the results may not be discarded, but an error up to 25% in wave height estimation is observed. This fact occurs because of the proximity of the theoretical estimation limit. So, a period margin must be established in order to avoid these cases.

As already said, the Parametric Method returned the full vector of parameters $x = [\omega_{m1}\ Hs_1 s_1\ \theta_{m1}\ \omega_{m2} Hs_2 s_2\ \theta_{m2}]^T$. However, for all experiments, one of the estimated significant height was indeed negligible, and a post-processor algorithm discarded the corresponding peak. This fact confirms the method ability to identify unimodal sea-states.

The spreading coefficient s is theoretically infinite for unidirectional sea states, like those generated in the towing tank. For all experiments conducted with wave incidence C, the estimated value was $s = 85$, which is high enough and the waves can be classified as unidirectional. For incidences A and B incidence the estimated spreading coefficient varied in the range 12–30, indicating some energy directional spreading. Fig. 22 contains the estimated wave spectrum contour plots for each incidence (A, B and C), confirming thus the spread computed for incidences A and B.

The wave reflection in the tank walls may explain this fact. Indeed, for incidence C, waves diffracted and reflected by the model propagate parallel to the tank borders. In A and B incidences, however, some diffracted and reflected wave components propagate perpendicularly to the walls, being reflected and reaching the ship model again. In these cases, a higher directional spreading is expected.

An analysis of all the results obtained shows that the Parametric Method produced estimates with errors smaller than 25% for wave significant height, 15% for peak period and 11° for mean direction. Figs. 23(a) and (b) show the results, showing a smaller dispersion in period when compared to height. Fig. 23(c) shows estimated directions for all valid experiments. Errors up to 11° in incidence B were observed.

Fig. 24 shows the estimated and measured wave power spectra for the experiment with full loaded ship, incidence A, test 3. It must be emphasized that the method produces good results even in the presence of a wave spectrum with a general shape different from the Pierson–Moskowitz spectrum. Indeed, it can be seen that the measured spectrum presents higher energy concentration than the estimated one. It resembles a JONSWAP spectrum (with $\lambda_1 > 1$), widely used to describe undeveloped sea states and swell waves. In this case the wave parameters were accurately estimated, with a 9% error in significant height and a −5% error in peak period estimates.

[2] The numerical analysis was not carried out for intermediate loading condition. The minimum peak period obtained for ballasted ship (10s) was also used for this condition.

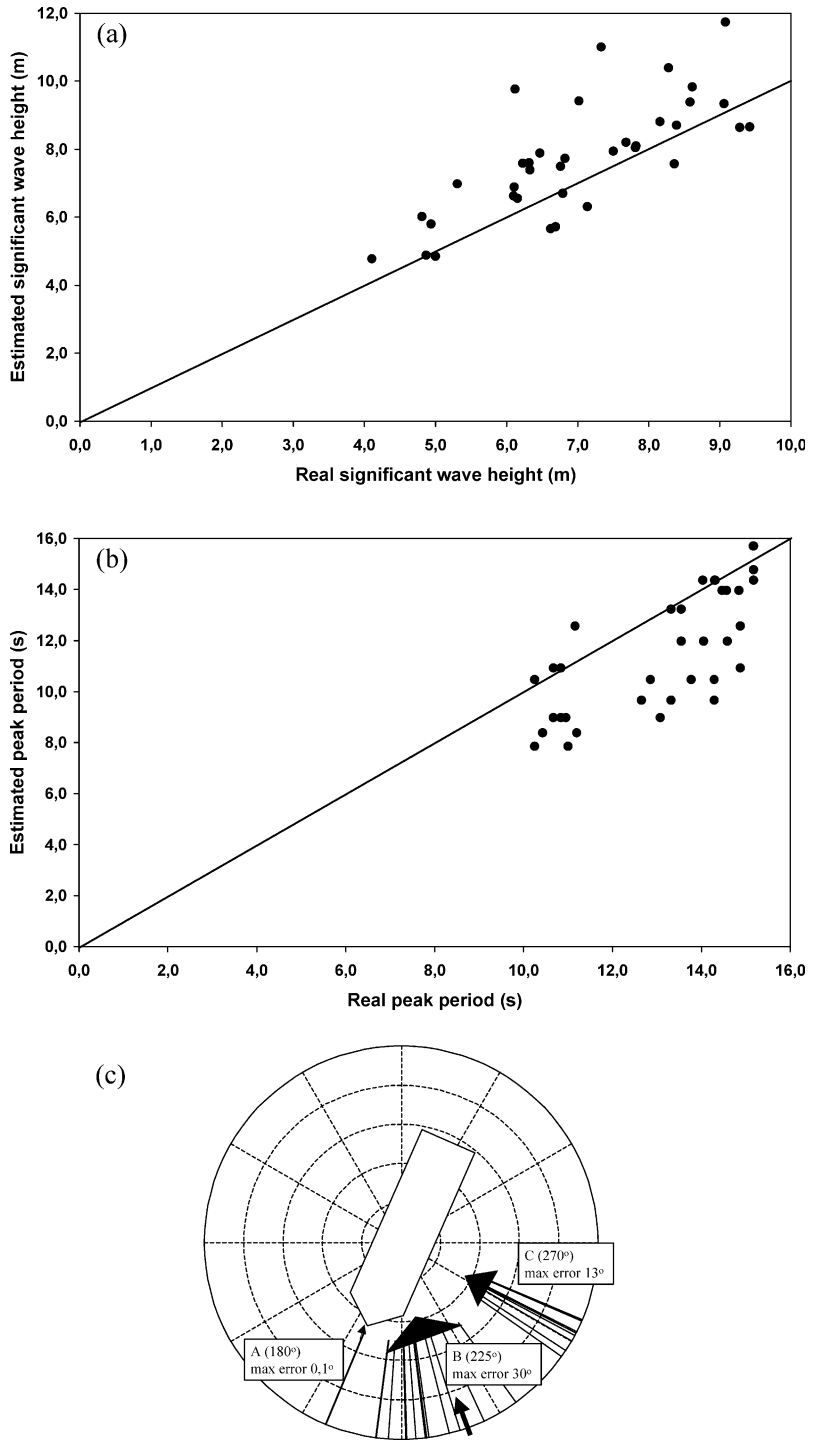

Fig. 25. Bayesian method results (a) Significant wave height; (b) Peak period; (c) Direction.

The experiments were also analysed using the non-parametric Bayesian Method previously mentioned. As it can be seen in Fig. 25, the estimation errors with the Bayesian Method are higher than those obtained with the Parametric Method, reaching 35% for significant height, 31% for peak period and 30° for direction.

These results suggest the superiority of Parametric Method in the present case.

6. Conclusions

The feasibility of wave spectrum estimation based on stationary ship motion measurements was analyzed in the present paper. Attention was given to the identification of critical problems that may arise when such methods are applied to large tanker ships. Such algorithms play an important role in feedforward controllers used in DP of ships.

The estimation methods depend on the previous knowledge of the response of the ship when subjected to waves expressed in the form of RAO's. Practical limitations mainly due to non-linear effects and variations in loading conditions appear in the application of the methodology to FPSO's.

This problem is partially addressed here by considering the variations of RAO's due to the uncertainty in ship loading—non-linear effects have not been taken into account in the paper. It was verified that roll motion is extremely sensitive to these variations, due to its resonant behavior. Then, unlike the usual applications of directional buoys, the use of sway instead of roll was proposed. This change can be made since, like roll, sway RAO is also an odd function of the incidence angle, preserving the directional information contained in the roll motion.

A Parametric Estimation Method was applied to a moored VLCC. The methodology was tested under typical wave conditions of the Campos Basin in numerical and towing-tank experiments.

First-order motion measurements are the basis for the estimation procedure proposed. So, the method will not work properly for high-frequency wave spectra, since they do not induce significant (first order) ship motions. Spectrum components with peak period smaller than a pre-calculated cut-off period cannot be accurately estimated. Numerical experiments corresponding to several peak periods were useful to determine the cut-off period for FPSO both in full loaded and ballasted conditions.

Other numerical experiments emulated critical 1 and 100 year unimodal Campos Basin sea condition, as well as typical bimodal states. For all cases, when the peak period was larger than the cut-off period, accurate estimates were obtained. Towing-tank experiments confirmed the previous numerical analysis.

Bayesian non-parametric method was also applied. It has shown to be strongly sensitive to uncertainties in RAO values, with worse results for both numerical and towing-tank experiments.

To close the paper, it has been shown that a wave spectrum estimation algorithm based on FPSO motions measurements is feasible, provided that some care is taken. Since the ship is being used as a wave sensor, its dynamics must be well known in order to perform good estimates of wave spectra.

Acknowledgements

This project was sponsored by Petróleo Brasileiro S/A (Petrobrás). Authors are grateful to Eng. Msc. André J.P. Leite, from Petrobrás and to the technical assistance of Professor José A. P. Aranha, from the Naval Arch. and Ocean Engineering Department of University of São Paulo. Third author acknowledges the financial support of Petroleum National Agency (ANP) and the fourth author thanks both to FAPESP (Proc. No. 97/04668-1) and to CNPq (Proc. No. 304071/85-4).

References

[1] Pinkster JA. Wave feedforward as a mean to improve DP. Proceedings of OTC 3057, Houston, 1978.
[2] Ewans KC, van der Vlugt T. Estimating bimodal frequency-direction spectra from surface buoy data recorded during tropical cyclones. J Offshore Mech Arctic Engng 1999;121:172–80.
[3] Muñoyerro MAA, Borge JCN. Directional wave navigation radar measurements compared with pitch-roll buoy data. J Offshore Mechn Arctic Engng 1997;119:25–9.
[4] Reichert K. WaMoS II: A radar based wave and current monitoring system. in Proceeding of the Ninth International Offshore and Polar Engineering Conference; 1999. pp. 139–143.
[5] Webster WC, Dillingham JT. Determination of directional seas from ship motions. in Proceedings of Directional Wave Spectra Applications'81; 1981. pp. 1–20.
[6] Hirayama T. Real-time estimation of sea spectra based on motions of a running ship (2nd report). J Kansai Soc Naval Arch 1987;204: 21–7.
[7] Iseki T, Ohtsu K. Bayesian estimation of directional wave spectra based on ship motions. Cont Engng Pract 2000;8:215–9.
[8] Benoit M, Goasguen G. Comparative evaluation of directional wave analysis techniques applied to field measurements. in Proceeding of the Ninth International Offshore and Polar Engineering Conference; 1999. pp. 87–95.
[9] Hogben N, Cobb FC. Parametric modelling of directional wave spectra. in Proceedings of 18th Offshore Technology Conference; 1986.
[10] Ochi MK, Hubble EN. Six parameter spectra. In: Ochi MK, Hubble EN, editors. in Proceedings of 15th Coastal Engineering Conference. 1976.
[11] Longuet-Higgins MS, Cartwright DE, Smith ND. Observations of the directional spectrum of sea waves using the motion of a floating buoy. Ocean Wave Spectra, Prentice Hall; 1963. pp. 111–136.
[12] Tannuri EA, Pesce CP, Donha DC. Assisted Dynamic Positioning System for a FPSO based on Minimization of a Cost Function. in Proceedings of Control Applications in Marine Systems Conference (IFAC-CAMS CD-ROM Glasgow, Escócia; 2001.
[13] N.A.B. Seixas, Clima de Ondas da Bacia de Campos: Análise dos Dados e Proposta de Parametrização. PhD Thesis, Observatório Nacional, Rio de Janeiro, 1997 (in Portuguese).
[14] Waals OF, Aalbers AB, Pinkster JA. Maximum likelihood method as a means to estimate the DWS and the mean wave drift force on a dynamically positioned vessel. Proceedings of OMAE'02, Norway; 2002.